EINDHOVEN UNIVERSITY OF TECHNOLOGY

Fast deposition of amorphous carbon films by an expanding cascaded arc plasma jet

Citation for published version (APA):
Buuron, A. J. M., Sanden, van de, M. C. M., Ooij, van, W. J., Driessens, R. M. A., & Schram, D. C. (1995). Fast deposition of amorphous carbon films by an expanding cascaded arc plasma jet. *Journal of Applied Physics*, *78*(1), 528-540. https://doi.org/10.1063/1.360637

DOI:
10.1063/1.360637

Document status and date:
Published: 01/01/1995

Document Version:
Publisher's PDF, also known as Version of Record (includes final page, issue and volume numbers)

Please check the document version of this publication:

• A submitted manuscript is the version of the article upon submission and before peer-review. There can be important differences between the submitted version and the official published version of record. People interested in the research are advised to contact the author for the final version of the publication, or visit the DOI to the publisher's website.
• The final author version and the galley proof are versions of the publication after peer review.
• The final published version features the final layout of the paper including the volume, issue and page numbers.

Link to publication

General rights
Copyright and moral rights for the publications made accessible in the public portal are retained by the authors and/or other copyright owners and it is a condition of accessing publications that users recognise and abide by the legal requirements associated with these rights.

• Users may download and print one copy of any publication from the public portal for the purpose of private study or research.
• You may not further distribute the material or use it for any profit-making activity or commercial gain
• You may freely distribute the URL identifying the publication in the public portal.

If the publication is distributed under the terms of Article 25fa of the Dutch Copyright Act, indicated by the "Taverne" license above, please follow below link for the End User Agreement:

www.tue.nl/taverne

Take down policy
If you believe that this document breaches copyright please contact us at:

openaccess@tue.nl

providing details and we will investigate your claim.

Download date: 19. Apr. 2025

Fast deposition of amorphous carbon films by an expanding cascaded arc plasma jet

A. J. M. Buuron[a] and M. C. M. van de Sanden[b]
Department of Physics, Eindhoven University of Technology, P.O. Box 513, 5600 MB Eindhoven, The Netherlands

W. J. van Ooij
Department of Materials Science and Engineering, University of Cincinnati, Cincinnati, Ohio 45221-0012

R. M. A. Driessens and D. C. Schram
Department of Physics, Eindhoven University of Technology, P.O. Box 513, 5600 MB Eindhoven, The Netherlands

(Received 29 April 1994; accepted for publication 13 March 1995)

Using an expanding cascaded arc plasma jet, amorphous hydrogenated and fluorohydrogenated carbon films were deposited on silicon, glass, and steel substrates at high rates of tens of nanometers per second and on large areas of up to 100 cm^2. The present work was aimed at depositing amorphous carbon films suited for optical and protective applications. Films deposited with the common argon/methane or argon/acetylene mixture tend to delaminate from the substrate when the film is thicker than about 1 μm. For this reason, also trials using other compounds like C_7H_8 (toluene), CF_4, and H_2, and mixtures of these, were carried out. Using toluene, several-μm-thick films with good adhesion to the substrate were deposited. With spectroscopic ellipsometry and infrared absorption spectroscopy optical parameters were obtained. Appropriate numerical models were developed for analyzing the data, taking into account interference fringes in the spectra due to multiple reflections in the thin film. The hydrogen and oxygen content in the films were determined with nuclear recoil techniques. Films deposited with the use of methane and acetylene are diamondlike with mainly sp^3 bonding types, and a hydrogen content ranging from 36 to 26 at. % (with a low oxygen contamination of 1–2 at. %). Films deposited with the use of toluene are more polymerlike, with also sp^1 and sp^2 bonding types. These films have a high hydrogen content (35 at. %), and can be partially oxidized (up to 13 at. %). In general, going from the polymerlike to the more diamondlike films, the refractive index increases from 1.3 to 2.2, and the band gap decreases from about 2 to 1 eV. By the admixture of hydrogen in the deposition plasma diamondlike films were produced with a larger band gap of 2.2 eV. The corrosion performance of the films was studied by storing them in a humidity cabinet. The corrosion resistance of films deposited with hydrocarbon/argon plasma mixtures appears to be limited. Thick films with a good corrosion resistance were produced by admixing a fluorine containing gas in the plasma. Analysis of the infrared absorption spectra showed that these films consist of amorphous fluorohydrogenated carbon. The presence of fluorine radicals in the plasma may lead to a chemically enhanced surface mobility, leading to a less porous film structure, and resulting in lower internal stresses. The growth rates and the corrosion performances of the films appear to be different for substrates of different types of steel. This may be attributed to different initial growth mechanisms, as a consequence of the difference in electrical and thermal conductivity of the two substrate types used here. © *1995 American Institute of Physics.*

I. INTRODUCTION

Plasma polymerization is a relatively new technique for surface modification and for deposition of amorphous hydrogenated carbon films (*a*-C:H films).[1–3] Compared to conventional gas-phase deposition methods, the plasma deposited films are known to be highly cross linked. In general the films are insoluble and pinhole free, and adhere well to most substrates. The *a*-C:H films have an extensive field of potential applications, because of their unique combination of specific properties such as hardness, low friction coefficients, chemical inertness, biocompatibility, and optical transparency in a wide wavelength range.[4] Some practical applications of *a*-C:H films are: overcoats on thin-film media for magnetic recording,[5] protective and antireflection coatings for optical devices working in the infrared,[6] insulating layers in electronic devices,[7] and coatings for biomedical purposes.[8]

The deposition rate with conventional plasma reactors like rf, microwave, or dc glow discharge reactors however are low (at maximum a few nanometers per second)[9,10] and hamper large-scale industrial applications of *a*-C:H films. In the last decade, at the Eindhoven University of Technology a method has been developed, using an expanding cascaded

[a]Present address: Laboratoire d'Aérothermique du Centre National de la Recherche Scientifique, 4ter Route des Gardes, 92190 Meudon, France.
[b]Author to whom correspondence should be addressed; Electronic mail: m.c.m.v.d.sanden@phys.tue.nl

 0021-8979/95/78(1)/528/13/$6.00 © 1995 American Institute of Physics

Downloaded 17 Mar 2005 to 131.155.108.252. Redistribution subject to AIP license or copyright, see http://jap.aip.org/jap/copyright.jsp

arc plasma jet, with which all types of carbon coatings are produced at deposition rates which are orders of magnitude higher[11–16] than with the conventional methods. For a-C:H films very high growth rates of up to 200 nm s^{-1} were achieved on areas of 100 cm^2. Conventional gases like methane and acetylene were admixed in the argon carrier gas. The band gaps of plasma deposited a-C:H films are mostly of the order of 1–2 eV. Further, the films tend to delaminate from the substrate at thicknesses larger than about 1 μm.[14]

In the present project, two sequences of deposition experiments were carried out. In the first sequence, acetylene (C_2H_2) and toluene (C_7H_8) were used as the hydrocarbon admixture and, in some trials, hydrogen (H_2) was added. The aim of this sequence was to find parameter settings with which thick films (3–4 μm) could be deposited, with a good adhesion to the substrate, and with optimum combinations of film properties aimed at optical applications. The optical parameters were determined using spectroscopic ellipsometry and infrared absorption spectroscopy. From the results of the latter, information on the predominant bonding types in the film was derived. Finally, the hydrogen and oxygen contents in the film were determined by nuclear scattering and recoil techniques.

In a second study the corrosion behavior of cold-rolled steel (CRS) and electrogalvanized steel (EGS), coated with a film of amorphous carbon was investigated. Research on the feasibility of depositing films with these qualities on steel for anticorrosion protection has increased rapidly in recent years. Recently, films deposited with trimethylsilane were reported to have a good corrosion performance.[17] These films were deposited in a rf parallel plate reactor, or in a dc bell-jar-type reactor. The deposition rates obtained (about 1 μm h^{-1}) were rather low. In the present study, the corrosion performance of carbon coatings deposited with the cascaded arc method are investigated with respect to substrate type and pretreatment and, type and flow rate of the admixed compound. Compounds admixed in the argon carrier gas were CH_4, C_2H_2, C_7H_8, and CF_4, and mixtures of these. In order to map the requirements on elemental composition and structure to this specific aim, the films were also studied using glow discharge optical spectroscopy (GDOS) and electron impedance spectroscopy (EIS). In some cases, also scanning electron microscopy (SEM), x-ray photoelectron spectroscopy (XPS), and time-of-flight secondary ion mass spectrometry (TOF-SIMS) were carried out. In this article we first address specific numerical models for analyzing the results of the optical diagnostics. In these models multiple reflection in a thin film is taken into account, and the effect of interference fringes is eliminated from the final results. Subsequently the deposition reactor, conditions, and the specifications of the various diagnostics are addressed. The results on the optical and protective properties of the films are discussed consecutively, both in relation to their elemental and structural composition.

II. ANALYSIS OF THE OPTICAL PROPERTIES OF THE FILMS

A. Spectroscopic ellipsometry

With *ex situ* spectroscopic ellipsometry the optical parameters of the deposited films, such as refractive index, absorption coefficient, and band gap were determined. The theory of this method has been described extensively.[18] Briefly, the method determines the change in polarization of linearly polarized light upon reflection on the system film substrate. This polarization change is expressed in the complex reflection ratio ρ:

$$\rho = R_p / R_s , \tag{1}$$

where R_p and R_s are the complex reflection coefficients for the light components polarized parallel and perpendicular to the plane of incidence, respectively. (For a semi-infinite medium they are directly equal to the Fresnel reflection coefficients.)[18] So ρ is a complex quantity and is generally expressed in the ellipsometric angles Ψ and Δ:

$$\rho = \tan(\Psi)\exp(j\Delta). \tag{2}$$

In measurement setups either a rotating analyzer or a rotating polarizer system is used. In both methods a periodic signal on the detection device arises. By Fourier analysis of this signal the ellipsometric Fourier coefficients a and b are determined. If the polarizer angle is set at 45°, these coefficients are related to the ellipsometric angles Ψ and Δ by the following relationships:

$$a = -\cos(2\Psi), \tag{3}$$

$$b = \sin(2\Psi)\cos(\Delta). \tag{4}$$

The parameters refractive index n and the extinction coefficient k, enter the formulas through the Fresnel reflection coefficients. The band gap can be determined using the Tauc relation[4,14,19]

$$\sqrt{\alpha E} = G(E - E_g) \tag{5}$$

with α the absorption coefficient (in cm^{-1}), $\alpha = 4\pi k/\lambda$; λ is the wavelength in vacuum of the incident light (in cm^{-1}), E is the photon energy (in eV), E_g is the band gap (in eV), G is a density-of-states coefficient (in $cm^{-1/2}$ $eV^{-1/2}$). Because of the limited thickness of the deposited layers, interference oscillations appeared in the signals as a function of wavelength, due to multiple reflections within the film. The method in which substrate and film are considered mathematically by one semi-infinite bulk medium[14,18] is no longer adequate. The system substrate layer has to be described by a multilayer system.[11,20] This prohibits a straightforward determination of n, k, and E_g using the equations above. The problem can be solved by reversing the solution method. This means that a fit procedure to the measured data can be applied, starting from a given set of thicknesses and optical parameters. From these values the expected values of the coefficients a and b can be calculated and by an iterative least-squares algorithm an optimum fit to the measured data can be obtained. Mathematically the multilayer system can be described most conveniently in terms of complex optical impedance factors for each layer. In the past, computer programs have been written to analyze the data of He-Ne *in situ* ellipsometry.[20] Recently,[21] the program has been adapted for calculations over a large wavelength range. A variable number of parameters can be included in the model: Often the system substrate layer is extended with a top layer, with different optical parameters. The theory of Bruggeman[22] sup-

Downloaded 17 Mar 2005 to 131.155.108.252. Redistribution subject to AIP license or copyright, see http://jap.aip.org/jap/copyright.jsp

plies a means for characterizing these surface parameters. The top layer is then described by a void fraction of 50% and a limited thickness (of some nanometers). However, it appeared that for the present amorphous carbon films, the implication of this top layer did not improve the fit quality significantly, so we omitted it in the fits. The following parameters were then included in the fit procedure.

(1) The thickness of the film d.
(2) The refractive index n, in first approximation taken constant over the wavelength range.
(3) The density-of-states factor G.
(4) The optical gap E_g.

Initial values for n, G, and E_g can be estimated from the amplitude of the fringes, and from the level and the slope of the a and b coefficients. The interference oscillations permit an initial film thickness estimate using

$$d=\frac{\lambda_i\lambda_{i+1}}{\lambda_i-\lambda_{i+1}}\frac{1}{2n}, \tag{6}$$

with λ_i and λ_{i+1} the wavelength of two successive interference maxima. As a measure for the quality of the fit the least-squares error function

$$\chi^2=\frac{1}{N}\sum_{i=1}^{N}(a_i^{\text{exp}}-a_i^{\text{calc}})^2+(b_i^{\text{exp}}-b_i^{\text{calc}})^2 \tag{7}$$

was adopted, with a and b the Fourier coefficients, N the number of data points, and the superscripts exp and calc denoting experimental and calculated a and b values, respectively. Weighing was not applied, because the absolute instrument noise (equal over the entire frequency interval) was predominant over the effect of the relative inaccuracies in a and b.

B. Infrared absorption spectroscopy

Infrared (IR) absorption spectroscopy supplies a means to determine the abundance of bonding types in a coating.[23,24] The transmitted intensity I_T through a layer of thickness d is described by the well-known exponential relationship

$$I_T=I_0\exp(-\alpha d), \tag{8}$$

with I_0 the intensity of the incident beam. The absorption coefficient α is related to the extinction coefficient k by $\alpha=4\pi k/\lambda$.

As in the case of the ellipsometric spectra, the measured IR absorption spectra are disturbed by interference oscillations, caused by multiple reflection in the layer. Assume that the incident light passes through a layer system air-substrate-coating-air subsequently. The various reflection and transmission coefficients on the interfaces have to be taken into account. To this end, the components of the system are denoted by the indices a, s, and c (and again a), respectively. The transmittance I_T/I_0 of the system under investigation, assuming perpendicular incidence of the light, is then given by (cf. Ref. 18):

$$\frac{I_T}{I_0}=\exp(-\alpha d_s)\|t_{as}\|^2\|t_{sc}\|^2\|t_{ca}\|^2\frac{\exp(-\alpha d)}{1-2\,\text{Re}[r_{ca}r_{cs}\exp(-j\phi)]\exp(-\alpha d)+\|r_{ca}\|^2\|r_{cs}\|^2\exp(-2\alpha d)}, \tag{9}$$

with r_{xy} and t_{xy} the (complex) reflection and transmission coefficients when the light encounters the interface from medium x to medium y, which are all related to n and k by the Fresnel relations; $\phi=4\pi nd/\lambda$ is the real part of the phase change on passing two times through the coating.

The ratio I_T/I_0 can be corrected for the attenuation of the beam through the substrate. This was done by measuring the transmission through an uncoated piece and a coated piece of silicon out of the same wafer. Using the ratio of the reference intensity I_U, transmitted through the uncoated substrate, and the incident intensity I_0,

$$\frac{I_U}{I_0}=\exp(-\alpha d_u)\|t_{as}\|^2\|t_{sa}\|^2, \tag{10}$$

in which d_u and d_s are the substrate thicknesses in the uncoated and coated substrate section, respectively ($d_u\approx d_s$ in general), the coating transmittance I_T/I_U can directly be deduced from Eq. (9). The applicability of an a-C:H layer as an optical coating is obvious. If the refractive index of the coating has a suited value, intermediate of that of the substrate and that of air, the transmittance of the system substrate coating will be higher than the transmittance of the bare substrate. All of the parameters (except the thicknesses) are a function of frequency (wave number), so $\alpha=\alpha_\nu$, etc. Using Eqs. (9) and (10) the coating transmittance $(I_T/I_U)_\nu$ can now be converted into the absorption coefficient α_ν. Two approaches are possible: When the thickness and refractive index of the coating (and substrate) are known, α_ν can be solved point by point by a simple computer iteration of Eq. (9). For a-C:H materials, the profile of α_ν in an absorption band can be fitted approximately by a Gaussian function.[25] When the thicknesses are not exactly known, the spectrum can be fitted starting from a suitable set of initial values for the thicknesses, refractive indices, and Gaussian absorption profiles in the vibrational bands. An estimate for the film thickness can be found using Eq. (6). A starting value for the refractive index can be estimated on basis of the amplitude of the interference fringes. The overall level mismatch caused by the difference d_s-d_u and, possibly by some residual overall absorption in the IR, can be adjusted by a flat or a linear background, giving one or two extra fitting parameters. Substituting the initial parameter estimates in Eqs. (9) and (10), the transmittance can be simulated over an entire wavelength range, and by a subsequent least-squares fit,

Downloaded 17 Mar 2005 to 131.155.108.252. Redistribution subject to AIP license or copyright, see http://jap.aip.org/jap/copyright.jsp

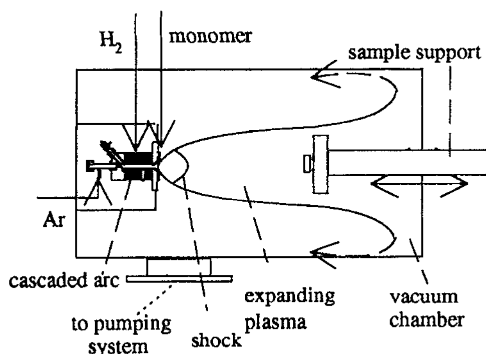

FIG. 1. Outline of the cascaded arc deposition reactor.

optimum values of the profiles of the absorption coefficient are obtained. In this way the Gaussian absorption bands are convolved towards the measured transmittance.

III. EXPERIMENT

A. The expanding cascaded arc set-up for deposition

In Fig. 1 an outline of the cascaded arc deposition reactor is shown. The main features of the expanding cascaded arc technique for deposition are the separation of the three phases production, transport, and deposition of active species. The argon carrier gas enters the cathode space of the cascaded arc at a pressure of about 0.5 bar. A plasma is generated in the channel of a cascaded arc and expands through the annular anode into a vacuum chamber (pressure of the order of 100 Pa). The monomer is injected in the anode and ionized and dissociated by the plasma. In the expanding plasma jet excited and ionized atomic and molecular radicals are transported towards the substrate, where deposition occurs at high rates. To maintain a low deposition temperature (necessary for a-C:H deposition), the substrate is water cooled. The reactor settings for a-C:H deposition are given in Table I. All flow rates are given in standard $cm^3 s^{-1}$, that is the flow rates are normalized on a pressure of 1 bar at room temperature and are denoted by means of {} braces.

As a specific parameter for characterizing the deposition with the expanding cascaded arc plasma jet, while varying a large number of parameters, often the inverse power-flow factor Q is used. It is similar to the inverse of the W/FM ratio, which is the common parameter in the case of stationary rf and dc deposition methods;[17] W is the power, F is the monomer flow rate, and M is the molecular weight of the monomer. The factor Q is defined as F/AW with F, the net carbon flow rate, A the argon flow rate, and W the power of the arc. In contrast to, e.g., Ref. 17, we cannot simply state that a high Q factor leads to a precursor-similar structure in the film. In our case the monomer dissociation degree is much higher, and various mechanisms contribute to the observed relationships between reactor settings and carbon film properties. As in our case the power and the argon flow were kept constant, we can present our results as a function of the hydrocarbon flow rate. The net carbon flow rate in a flow of 0.151 ml $min^{-1} C_7H_8$ is equal to the net carbon flow rate in a flow of 2 $cm^3 s^{-1}$ C_2H_2. A flow rate of 1 $cm^3 s^{-1}$ C_2H_2 is equivalent to a Q factor of $\sim 5\times10^{-6}$ W^{-1}. More details on the deposition reactor, the reactor settings, and the relations with the deposited materials are given elsewhere.[14,15]

TABLE I. The reactor settings and flow rates used for a-C:H,F deposition.

I_{arc} (A)	50
V_{arc} (V)	90
{Ar} ($cm^3 s^{-1}$)	100
{C_xH_y} ($cm^3 s^{-1}$)	0.36–10.9
{C_7H_8} (ml min^{-1})	0.068–0.378
{H_2} ($cm^3 s^{-1}$)	3, 14
{CF_4} ($cm^3 s^{-1}$)	0.4, 0.6
p_c (Pa)	22, 100
T_s (°C)	30–210
d_{n-s} (cm)	70

In the present project, two sequences of deposition experiments were carried out. The first sequence was aimed at optimizing the properties of the films suited for optical applications, the second at depositing films on steel substrates providing a good anticorrosion protection. A major demand for the films in both sequences was that they have a good adhesion to the substrate.

In the first sequence acetylene (C_2H_2) and toluene (C_7H_8) were used as admixtures. With acetylene a series of thin ($\sim$500 nm) films was deposited, in order to update the results found in the past.[14,15] In a second series, thick films (>1 μm) with a good adhesion to the substrate were deposited with the use of toluene. The most promising trials of both series were repeated with admixture of hydrogen as an extra feed gas in order to try and deposit more diamondlike films with enhanced sp^3 bonding. Each trial batch consisted of one B-doped ⟨100⟩-silicon substrate (2.5×2.5 cm^2) and one glass substrate (Menzel–Gläser microscopy glasses; 3×1 in.). The diagnostics were all carried out on the coatings on the silicon samples; the glass samples were mainly meant for a qualitative judgment of the adhesion and the transparency of the coating. The range of the applied reactor settings is given in Table I, with the notice that in this sequence the chamber pressure was always 100 Pa.

In the second main sequence, the corrosion-performance study, films were deposited using various hydrocarbon flow rates, and with CF_4 as an extra admixture. In each batch, substrates of two types of steel, each with dimensions 5×5 cm^2 were placed: The steel types used were cold-rolled, low carbon steel (CRS) of automotive grade and electrogalvanized steel (EGS), both manufactured by Armco Research and Technology (Middletown, OH). To facilitate various film diagnostics, also a substrate of silicon was added. In this second sequence the chamber pressure was reduced to 22 Pa, in order to enlarge the deposition area.

B. Adhesion improvement by pretreatment

Adhesion of a-C:H films to the substrate is a major issue in the study of the applicability of these films for protective purposes. A distinction can be made between the polymer-like, hydrogen-rich films, which are deposited in low Q-factor trials, and the diamondlike, hydrogen-lean films at the high-Q side of the reactor parameter range.[12,15] In gen-

Downloaded 17 Mar 2005 to 131.155.108.252. Redistribution subject to AIP license or copyright, see http://jap.aip.org/jap/copyright.jsp

TABLE II. Survey of the trials for the optical applications; {CH_4}, {C_2H_2}, {C_7H_8}, and {H_2}, flow rates; d and R_d, film thickness and growth rate on silicon as obtained from the ellipsometric fits; t_d, duration of deposition; T_s, deposition temperature; p_c, chamber pressure. $p_c = 100$ Pa. All other reactor settings are given in Table I.

Sample	{C_2H_2} ($cm^3 s^{-1}$)	{C_7H_8} (ml min^{-1})	{H_2} ($cm^3 s^{-1}$)	d (nm)	R_d (nm s^{-1})	t_d (s)	T_s (°C)
E8	⋯	0.068	⋯	⋯	⋯	180	190
E9	⋯	0.151	⋯	720	6.0	120	180
E10	⋯	0.227	⋯	1660	5.5	300	200
E11	⋯	0.302	⋯	1730	9.6	180	210
E12	⋯	0.378	⋯	2300	15	150	⋯
F1	0.36	⋯	⋯	370	2.9	125	160
F2	0.90	⋯	⋯	370	6.2	59	150
F3	1.90	⋯	⋯	395	14	29	110
F4	3.6	⋯	⋯	265	19	14	70
F5	6.6	⋯	⋯	310	44	7.3	30
F6	10.9	⋯	⋯	245	61	4.0	30
G1	10.9	⋯	14	500	15	32.5	50
G2	6.6	⋯	14	50	2.0	26	50
G3	3.6	⋯	14	49	1.0	50	50
H2	⋯	0.151	3	2380	9.6	240	⋯
H3	⋯	0.151	3	8120	9.0	900	⋯

eral polymerlike films are soft and adhere reasonably well to the substrate. Using gaseous precursors like CH_4 and C_2H_2, with our method this is valid for thicknesses of up to about 1 μm.[14] Particularly the diamondlike films contain internal stresses,[19] and have a tendency to delaminate at thicknesses of only a few hundreds of nanometers.

It is well-known that a thorough cleaning of the substrate before depositing an a-C:H layer is essential for the adhesion of the film. For the glass and silicon substrates 5 min ultrasonic cleaning in an organic solvent (trichloroetylene) was carried out. For the CRS and EGS substrates this treatment must consist of a few stages. In order to remove stamping oil, the substrates were first cleaned ultrasonically in trichloroetylene (purity >99.5%) for 5 min. As a second stage, the steel substrates were cleaned in a 100/5 Ar/H_2 plasma for 5 min, with a substrate temperature rising to ~300 °C. In recent studies[17,26] it was found that optimum cleaning was achieved by cleaning in a pure hydrogen plasma for 60 min. This may be preceded by cleaning in an oxygen plasma for 2 min. The oxygen plasma is able to remove organic contaminations on the substrate partially and by the hydrogen plasma the residues are cross linked which improves the sticking to the substrate. An important finding is also that on the EGS substrates the hydrogen plasma is able to remove the (insulating) oxide layer completely, while it does not remove the oxide on the CRS substrates.

The deposition on the steel substrates was divided into two stages. In the first stage of the deposition, the substrate was dc negatively biased for 20 s. This can be considered as a third pretreatment stage, in which it was attempted to create an intermediate steel-carbon layer. The bias potential was limited to ~−200 V in order not to damage the growing layer. On the other hand, it is not sure whether this bias value was high enough to really implant the ions.[27,28] After switching off the bias the actual deposition was carried out during some tens of seconds.

C. Film diagnostics

For determining the optical parameters of the film, ellipsometry measurements were carried out by the group Surface Physics of the Department of Physics of the Eindhoven University of Technology. The setup used[29] was practically identical to the one previously described.[30] A rotating polarizer system (static analyzer at 45° orientation) with a stagnant cascaded arc as a high-intensity light source was used. The angle of incidence was 68.3°, and wavelength dependent signal detection occurred by means of a photodiode array. The ellipsometric Fourier coefficients a and b were determined over the wavelength range from 300 to 1100 nm (from 4.5 to 1 eV).

For determining the bonding types in the film, IR spectra were recorded with a Bruker IFS 66 Fourier transform interferometer, with a resolution of 4 cm^{-1}, using again a stagnant cascaded arc as a light source.

In order to determine the hydrogen content and possible oxygen incorporation in the films (both bonded and not bonded), nuclear recoil techniques were carried out using a beam of high energy α particles, produced by the AVF cyclotron of the Department of Physics of the Eindhoven University of Technology. In each measurement two techniques were used simultaneously, nuclear backscattering for calibration purposes and (noncoincident) elastic recoil detection analysis (ERDA) for the actual concentration determination. Two different experimental configurations, beam energies and detection methods were used, for the detection of the heavy elements oxygen and carbon, and the light element hydrogen, respectively. More information on these techniques can be found in the literature.[31,32]

The diagnostics for testing the corrosion resistance of the films were all carried out by Armco Research and Technology and related laboratories.

Downloaded 17 Mar 2005 to 131.155.108.252. Redistribution subject to AIP license or copyright, see http://jap.aip.org/jap/copyright.jsp

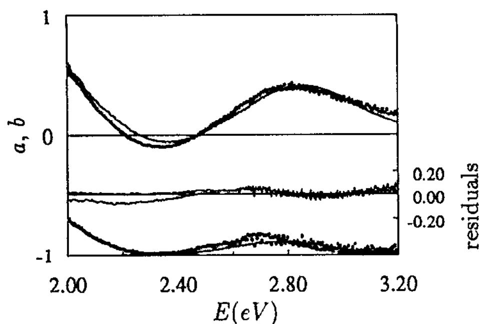

FIG. 2. Measured and fitted ellipsometric Fourier coefficients (trial F5).

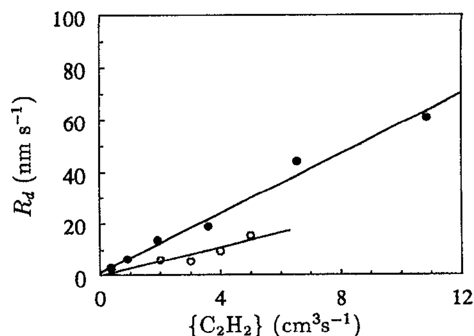

FIG. 3. Deposition rate R_d as a function of hydrocarbon admixture; ● C_2H_2, ○ C_7H_8. The flow rate of toluene is displayed as equivalent acetylene flow.

Glow discharge optical spectroscopy (GDOS) was used for depth profiling of the films. In the GDOS diagnostic (cf., e.g., Ref. 33) the film is sputtered by a beam of high energy argon ions. Typical operating parameters are a voltage of 700 V and a current of 30 mA. The device used is a LECO GDS-1000 glow discharge spectrometer. A qualitative picture of the sputtered elements is obtained by observing the optical emission of the glow discharge. In this way a depth profile of the elements in the film is obtained as a function of time. It should be noted that the GDOS technique has a widely varying sensitivity for the different elements and can only be used for a qualitative analysis. For instance, it appears to be very insensitive to hydrogen. On the other hand it is known that small amounts of nitrogen in a plasma can lead to strong optical emission bands.

The corrosion performance of the films was tested qualitatively by storing them in a humidity cabinet (85% relative humidity, 60 °C) for 96 h.

EIS[17,26] yields information on the barrier properties of the films. This is a relatively novel method. The most important parameter is the pore resistance R_{po}. This quantity is equal to the modulus of the impedance of the system in the limit of zero frequency. This parameter is a direct measure for the porosity of the layer and consequently for the corrosion performance.

Preliminary TOFSIMS measurements were carried out on one sample in order to investigate the possible merits of this technique for the analysis of amorphous carbon films. The measurements were performed on a Kratos PRISM instrument.[34]

SEM was applied for studying the morphology.

IV. RESULTS

A. The properties of *a*-C:H films aimed at optical applications

1. Results of the spectroscopic ellipsometry and the infrared absorption spectroscopy

In Table II a survey of the coatings studied for their suitability for optical purposes is given. In Fig. 2 an example of a representative fit to the measured *a* and *b* coefficients is shown. It can be observed that the fit is satisfactory and that the model is adequate for the present purpose. The fit can probably be improved by using the program options of a frequency dependence of the refractive index, and of the top layer. The drawback is that the number of fit parameters increases. Another disturbing factor may be the fact that the spectroscopic data are very sensitive to a slight error in the angle of incidence.[18] Moreover, the validity of the Tauc relation is limited. This hinders the selection of the appropriate wavelength range, since this depends again on the (unknown) band gap. So future refinements on the application of this method are desirable. Nevertheless, the accuracy of the fit was sufficient to obtain approximate results on the thicknesses, band gaps, and refractive indices of the films.

In Fig. 3 the deposition rate as function of the flow rates is shown, as obtained from the best-fit thickness of the ellipsometric data. It can be observed that the deposition rate increases almost linearly with the hydrocarbon flow rate up to large values. The area of deposition was ~100 cm^2. In Fig. 4 the refractive index and the band gap are shown as a function of the flow rates of acetylene and toluene. The values of G were in the order of 150–300 cm$^{-1/2}$ eV$^{-1/2}$. The value of 280 cm$^{-1/2}$ eV$^{-1/2}$, commonly reported for amorphous carbon films[4] was not always appropriate. For acetylene the same tendencies for the refractive index and the band gap as found in the past[15] were obtained. For toluene, the refractive index is hardly dependent on the flow rate. The band gaps actually found are somewhat higher and may be more realistic, because most of the films are transparent for

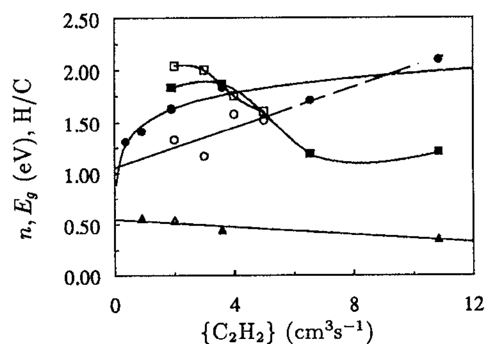

FIG. 4. ●, the refractive index n, ■ band gap E_g, and, ▲ H/C ratio, as a function of the equivalent (acetylene) flow rate; solid symbols, acetylene; open symbols, toluene.

Downloaded 17 Mar 2005 to 131.155.108.252. Redistribution subject to AIP license or copyright, see http://jap.aip.org/jap/copyright.jsp

TABLE III. Peak assignment for the infrared C-H absorption bands observed in our a-C:H layers. The first block gives the stretching vibrations, the small second block gives the observed bending vibrations (from Ref. 35).

Band	Frequency (cm^{-1}) Polymerlike	Diamondlike	Assignment
H1	3300	3300	sp^1CH
H5	···	2970	sp^3CH_3
H7	2920	2920	sp^3CH_2
H8	2920	···	sp^3CH
H9	···	2875	sp^3CH_3
H10	2850	2850	sp^3CH_2
C2	1620	1600	sp^2C=C olefinic
C3	1580	1580	sp^2C=C aromatic
B1	1370	1370	sp^3CH
B2	1450	1450	$sp^{2,3}CH_2$

red and orange light. The band gap decreases with an increasing hydrocarbon flow rate. For toluene the same tendency can be noted.

For optical purposes the ratio of the diamondlike sp^3 bonding and the polymeric and graphitic sp^1 and sp^2 bonding types is of utmost importance. Particularly, the presence of delocalized π electrons in aromatic rings (e.g., in graphite) will reduce the band gap drastically. With infrared absorption spectroscopy the prevalent bonding types in the film can be determined. Extensive studies of the assignment of the IR absorption bands observed in a-C:H layers were carried out by Dischler *et al.*[10,24,35] Table III gives a selection, summarizing the C—C and C—H bonding types observed in our a-C:H layers.

Using the method described in Sec. II B, the IR absorption bands were determined absolutely by convolving them towards the measured IR absorption spectra. In Fig. 5 a typical spectrum of an a-C:H film is shown over a wide wave number. The power of the fit method in eliminating the interference fringes is also demonstrated. The results of the fits of the various trials can be summarized using band integrated intensities (or ratios) and band widths as relevant parameters.

It appeared that for all films deposited with acetylene (sequence F, Table II), only the sp^3 bands around 2900, 1450, and 1370 cm^{-1} are present. This confirms the finding[12]

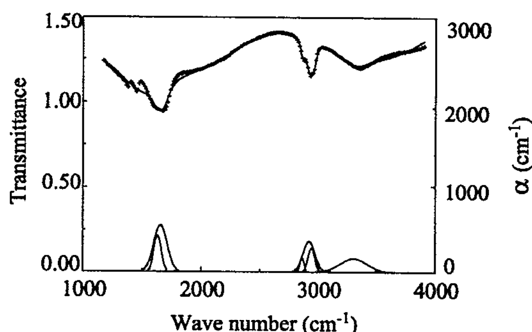

FIG. 5. Example of a wide wave-number-range fit of interference fringes and the most prominent absorption bands of an a-C:H film (trial E11).

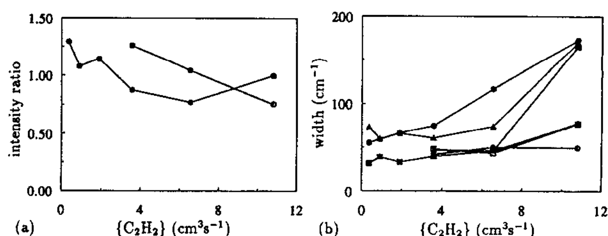

FIG. 6. (a) ● Integrated intensity ratios A_{2920}/A_{2970} and (b) ■, ●, ▲ widths of the 2875, 2920, and 2970 cm^{-1} band, respectively, as a function of the acetylene flow rate; Solid symbols: no hydrogen addition; open symbols: with 14 standard $cm^3\,s^{-1}$ H_2 addition.

that films deposited with our technique, using acetylene, are predominantly diamondlike. In this case the ratio of the band integrated absorption coefficient of the 2920 cm^{-1} $sp^3CH_{1,2}$ and of the 2970 cm^{-1} sp^3CH_3 band should give an indication for the degree of cross linking (more C—C bondings). In Fig. 6(a) these band integrated absorption coefficient ratios are given as a function of the acetylene flow rate (solid symbols). No clear dependence of this ratio on flow rate can be observed. This may be due to the thickness differences of the films and the relative influence of a top layer and a substrate-film sublayer of different composition. In Fig. 6(b) the band widths are given as a function of the acetylene flow rate. The widths of the bands increase with increasing flow rate, indicating a harder (more diamondlike) film.[35] The top values of the bands all decrease, for example the maximum of the 2920 $sp^3CH_{1,2}$ cm^{-1} band decreases from about 1000 to about 300 cm^{-1}.

Preliminary trials (sequence G) were carried out in order to try and improve the optical properties of the deposited films, by admixing various amounts of hydrogen in the plasma, following the experiences from crystalline diamond deposition trials.[15] In Fig. 6 the results for three values of the acetylene flow rate, upon addition of 14 $cm^3\,s^{-1}$ H_2 are shown (open symbols). It can be observed that the ratio of the integrated intensities of the $sp^3CH_{1,2}$ and sp^3CH_3 bands increases, that is the films become more diamondlike with an increasing H/C ratio in the plasma. Only for one film (G2) also the ellipsometric spectrum was recorded. The refractive index appeared to be low (1.5) but the band gap was enlarged from 1.2 to 1.6 eV (with $G=280$ $cm^{-1/2}\,eV^{-1/2}$). The growth rate was reduced to about 2 nm s^{-1}, so the hydrogen flow rate may have to be optimized. This result looks promising and future trials with this mixture are recommended.

Analyzing the IR spectra of the films deposited with toluene as an admixture (sequence E, Table II), it appeared that these films all have a polymeric character. Besides various sp^3CH_x bands also the aromatic and olefinic sp^2C=C bands at 1580–1620 cm^{-1} and the sp^1CH band at about 3300 cm^{-1} can be observed (cf. Fig. 5). Besides the absorption coefficient ratio of the 2920 $sp^3CH_{1,2}$ cm^{-1} band and the 2970 cm^{-1} sp^3CH_3 band, in this case also the ratios with the sp^1CH band at 3300 and the sp^2C=C bands around 1600 cm^{-1} give an indication for the degree of cross linking. In Fig. 7(a) these ratios are given as a function of toluene flow rate. It is clear that the films become more diamondlike

Downloaded 17 Mar 2005 to 131.155.108.252. Redistribution subject to AIP license or copyright, see http://jap.aip.org/jap/copyright.jsp

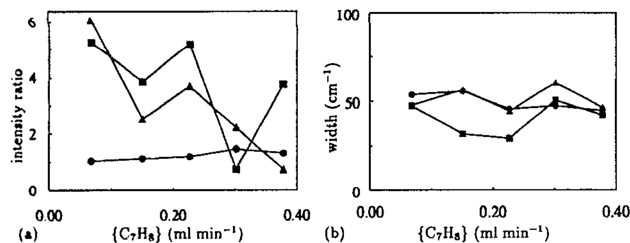

FIG. 7. (a) Integrated intensity ratios and (b) widths as a function of toluene flow rate. Legend for Fig. (a): ●, A_{2920}/A_{2970}, ■ $A_{1580}/A_{2920+2970}$, ▲ $A_{3300}/A_{2920+2970}$. Legend for fig. (b): ■, ●, ▲ widths of the 2875, 2920, and 2970 cm^{-1} band, respectively.

with higher flow rates. In this case, the widths of the bands [Fig. 7(b)] do not show a clear dependence on the flow rate. Simultaneously the absolute values of all the absorption coefficients appeared to decrease with increasing flow rate. For example, the maximum absorption coefficient of the 2920 $sp^3CH_{1,2}cm^{-1}$ band decreases from about 600 to about 300 cm^{-1}. This may indicate that the layers become also less dense with increasing flow rate. So the observed tendencies may be not always very pronounced, due to a combination of physical effects.

A substantial improvement was again obtained by admixing hydrogen (using a small amount, taking into account the lower deposition rate for toluene). Two trials (H2 and H3) were carried out with an admixture of 3 $cm^3 s^{-1}$ H_2 and 0.151 ml min^{-1} C_7H_8 into the plasma. After the test H2, trial H3 was carried out aimed at depositing a thick (and protective) film, with good optical properties and a good adhesion. A deposition period of 15 min resulted in a thick (8.1 μm) film with a good adhesion to glass and silicon substrates.

In the IR absorption spectrum of the film, the sp^1CH band at about 3300 and the sp^2C═C bands around 1600 cm^{-1} were not present anymore. The admixture of hydrogen favors the formation of a diamondlike (sp^3 dominated) structure. Due to the difference in deposition period, the two films H2 and H3 have widely different thicknesses and transmittances. However, the absorption band coefficients of both films H2 and H3 appeared to be identical, at maximum approximately 2000 cm^{-1} for the 2920 $sp^3CH_{1,2}$ cm^{-1} band, confirming both the reproducibility of the deposition method and the accuracy of the convolution method.

From the ellipsometry data a refractive index of 1.55 and an optical band gap of 2.2 eV (with $G=600$ $cm^{-1/2}$ $eV^{-1/2}$) were determined. Optically the films are yellow transparent, confirming this value for the optical gap. Similar results have been reported in Ref. 36.

In principle the exact number density of bondings C_H (and also C_c) per cm^3 can be calculated from the band integrated absorption coefficient, and in this way a density estimation should be possible. To this end following formula (e.g., Ref. 37) can be used

$$C_H=A_s\int \frac{\alpha_\nu}{\nu}\,d\nu, \tag{11}$$

with A_s the inverse absorption cross section and ν the frequency (or, equivalently, the wave number) of the incident light. For the stretching modes of the three CH_x ($x=1$, 2, and 3) bonding states, an average value of $A_s=10^{21}$ cm^{-2} can be adopted.[37] For our coatings, C_H number densities of the order of 5×10^{22} cm^{-3} are then obtained. In Ref. 10 densities for a-C:H layers of typically 1.5–1.8 g cm^{-3} are reported, with comparable values for the band integrated C-H absorption coefficients. The C-C vibrations are lying in the range 700–1500 cm^{-1},[35] and in the actual measurements we could not resolve these, probably due to the low infrared absorption cross-section for this type of bonding.

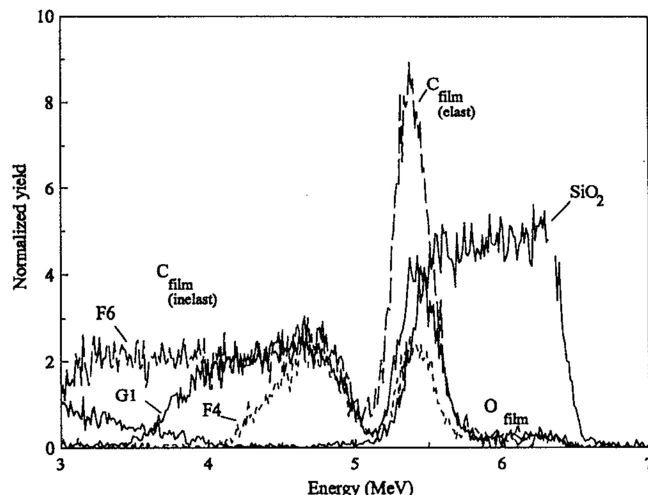

FIG. 8. Carbon-oxygen ERDA spectra of samples F4, F6, and G1. The SiO_2 signal is used for calibration.

2. The atomic H/C and O/C ratios as determined by the nuclear recoil techniques

In Fig. 8 some typical carbon/oxygen-ERDA spectra are shown. The high intensity peak at about 5.4 MeV is caused by elastically recoiled C atoms which pass through the thin foil detector and only reflect a relative impression of the layer thickness. Depth profiling is obtained by the spectra of the inelastically recoiled carbon atoms (with emission of gamma radiation). These exhibit an intensity distribution independent of the recoil energy, showing that the bulk of the film is homogeneous over the thickness. The slowly decreasing low-energy edge of especially the carbon signals may be due to layer thickness or density variations in the substrate-film interface (except the gradual decrease observed for the reference oxide, which is due to the variation of the cross-section with energy). From the ERDA measurements the total numbers of carbon, oxygen, and hydrogen atoms per cm^2 and their ratios were obtained. Measurements were carried out only for a selected number of the deposition trials. It should be noted that for the actual specific measurement technique special thin films of about 50 nm were required. In Table IV the results are summarized. So the trials in column I of Table IV are reproductions of those in Table II, with a very short deposition time (a few seconds). The ERDA measurements for carbon and oxygen were carried out one day after the deposition of the films. Also the hydrogen content of samples E9, H2, and F1 was measured on the same day.

Downloaded 17 Mar 2005 to 131.155.108.252. Redistribution subject to AIP license or copyright, see http://jap.aip.org/jap/copyright.jsp

TABLE IV. Results of the ERDA measurements; flow rates C_7H_8 in ml min^{-1}, other (gas) admixtures in $cm^3 s^{-1}$.

Sample	Feed gas +flow rate	C number (10^{15} cm^{-2})	O number (10^{15} cm^{-2})	H number (10^{15} cm^{-2})	O/C	H/C
F1	0.9 C_2H_2	300	4.5	168	0.015	0.56, 0.57
F4	3.6 C_2H_2	830	25	374	0.030	0.45
F6	10.8 C_2H_2	2400	36	860	0.015	0.36
G1	10.8 C_2H_2+14 H_2	1600	43	400	0.027	0.25
E9	0.151 C_7H_8	290	64	156	0.22	0.54
H2	0.151 C_7H_8+3 H_2	480	37	210	0.076	0.44

The hydrogen content of the other samples were measured three months later. As a check the H/C ratio of sample F1 was determined in both measurement series. The H/C ratios were 0.56 and 0.57, respectively, showing the good reproducibility of the results of this technique and indicating that the hydrogen content in the films does not change substantially with time. It can be observed that with increasing acetylene flow (F1 through F6) the hydrogen contents in the films decrease, indicating an increasing diamondlike character, in agreement with the IR results and Refs. 12 and 15. The absolute values of the H/C ratio are much lower than in Ref. 12, where a different measurement technique was applied. The actual values around 0.5 are more realistic and of the same order as the ones reported in other literature.[10] In general the oxygen content in the films is small. The high oxygen content (13 at. %) for sample E9, deposited using toluene may be due to the relatively large amount of double and triple carbon bonds in the deposited film. By exposure to air these may be oxidized. Another possibility is that the oxygen was already dissolved in the (liquid) toluene.

In Ref. 23 it is reported that it is possible to relate the C-H number densities as obtained by the IR transmission measurements using Eq. (11) and the H/C ratio as determined by the ERDA measurements quantitatively to each other. The following relationship is given:

$$\int \frac{\alpha_\nu}{\nu} d\nu \approx 96 \left(\frac{H}{C} \right)_{\text{ERDA}} . \tag{12}$$

For our films this relationship appears to be only roughly valid. This may be due to the fact that with ERDA also the unbonded hydrogen is detected.

B. The parameters of *a*-C:H,F coatings for anticorrosion protection

1. Introduction

Trials aimed at producing a good anticorrosive film were carried out, using both hydrocarbons and fluorocarbons as an admixture. Films produced with the latter admixture are known to exhibit a moisture-repulsive behavior[38] which might imply also a good corrosion performance. In Table V a survey of the most important trials is given. The films of trials D5 through D12 were deposited on large steel substrates (5×5 cm^2) and these were analyzed by several techniques. Only for D7 a stable thermocouple temperature measurement was obtained, but the other temperatures can be estimated to be of the same order (depending on deposition time).

2. Results of the GDOS

In Fig. 9 a typical GDOS spectrum for a film deposited on a CRS substrate is shown (trial D7). From correlating the GDOS sputter time with the thickness of the layer as estimated by a SEM photograph, it could be deduced that about 1 μm of an amorphous carbon film is sputtered in about 35 s. Using the fact that the sputter rate is approximately constant for films of the same type, estimates for the growth rate of all of the films were deduced. In Fig. 10 (cf. Table V) the obtained growth rates on the CRS substrates are given as a function of the hydrocarbon flow rate. The GDOS spectrum reveals some specific features. The peak in the first seconds is an artifact during stabilization of the ion beam. Contaminations of oxygen, nitrogen, and iron can be observed. The

TABLE V. Survey of the trials for the protective applications; {C_2H_2}, {C_7H_8}, and {CF_4}, flow rates; d and R_d, film thickness and growth rate from the GDOS experiments; t_d, duration of deposition; V_{bias}, negative bias voltage applied during the first 20 s of the actual deposition; T_s, deposition temperature; p_c, chamber pressure. $p_c=22$ Pa. All other reactor settings are given in Table I.

Sample	{C_2H_2} ($cm^3 s^{-1}$)	{C_7H_8} (ml min^{-1})	{CF_4} ($cm^3 s^{-1}$)	d (CRS, EGS) (nm)	R_d (CRS, EGS) (nm s^{-1})	t_d (s)	V_{bias} (V)	T_s (°C)
D5	3.0	···	···	610, 450	12, 9	50	−70	70
D6	6.0	···	···	910, 850	30, 28	30	−110	···
D7	3.0	···	0.6	1060, 830	21, 17	50	−50	110
D8	6.0	···	0.6	1000, 830	22, 19	45	−50	···
D9	1.5	···	0.6	480, 270	8, 4	60	−100	···
D10	···	1.0	···	540, 450	9, 7	60	0	···
D11	···	0.4	···	1440, 2090	36, 52	40	−800	···
D12	···	0.4	0.6	60, ···	0.5, ···	120	−10	···

Downloaded 17 Mar 2005 to 131.155.108.252. Redistribution subject to AIP license or copyright, see http://jap.aip.org/jap/copyright.jsp

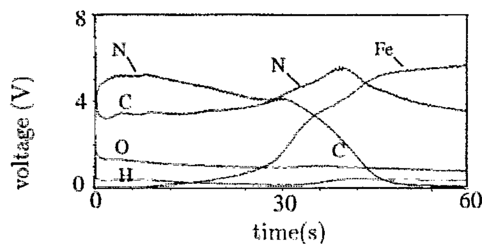

FIG. 9. Typical GDOS spectrum of a coated CRS substrate (D7).

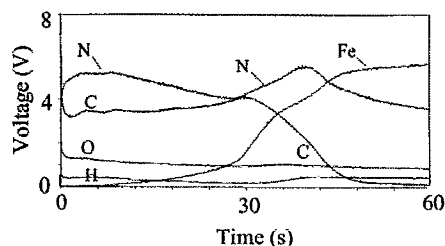

FIG. 11. Typical GDOS spectrum of a coated EGS substrate (D7).

former are probably due to residual gases in the deposition chamber. The latter is an indication of a porous film. Physical sputtering of iron during the deposition of the film is very unlikely, in view of the low bias potential and hence ion energy. Further, it can be observed that the substrate film interface appears diffuse. This may be a consequence of the third pretreatment, the bombarding of the substrate with carbon ions, but possibly it is an artifact of the method (rapid simultaneous sputtering of film and substrate). All the films deposited on CRS substrates showed a spectrum similar to the one of Fig. 9, with slight variations in contaminations signals. In films deposited at a higher chamber pressure, these signals were relatively lower (as expected).

In Fig. 11 the spectrum of the film grown simultaneously on the EGS substrate is shown. Besides the contaminations already mentioned, a very interesting feature can be observed in the substrate-film region. The carbon signal shows a pronounced rise. This may be an artifact due to the conductivity of the substrate, but more likely it is an indication for the presence of a substrate-material dependent interfacial layer. This hypothesis is supported by the fact that the film deposited on EGS was always thinner than the one deposited on CRS (in the same trial). As the absolute value of this difference is approximately constant, it points to some kind of incubation time before the growth starts on zinc. These two phenomena indicate that the initial growth may be different on CRS and EGS substrates, as a consequence of the difference in electrical and thermal conductivity of the substrate. Subsequently, the initial growth mechanism may have influence on the growth mode of the bulk of the film.

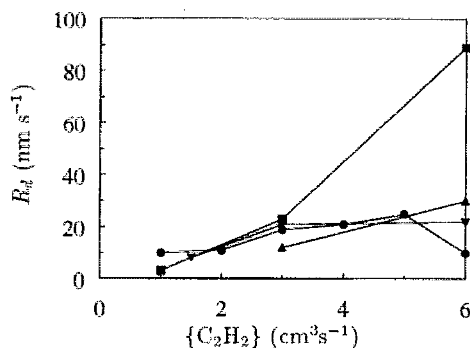

FIG. 10. Growth rate (on CRS substrates) as a function of various gas admixture flow rates, ■ C_2H_2, ● CH_4 (p_c=100 Pa); ▲ C_2H_2, ▼, C_2H_2+0.6 CF_4 (p_c=22 Pa).

3. Results of the corrosion performance studies

In Fig. 12 the qualitative results of the corrosion tests are shown. Bare CRS substrates show severe corrosion in this test [Fig. 12(d)]. The corrosion performance of films deposited with an argon/hydrocarbon plasma (e.g., D11) is moderate, particularly of the thicker films. Most probably not the thickness but the adhesion is a very important factor, in addition to the film composition. Samples D7 and D9 showed a good corrosion resistance. These were films produced with acetylene, with additional admixture of CF_4. Preliminary XPS measurements indicate a content of 10 at. % F, 3% N, 12% O, and 75% C for sample D7.[39] In Fig. 13 the IR transmission spectrum of a typical a-C:H,F film (trial D9; on the silicon reference sample) is given. It appears that besides low-amplitude C—H bands also the C—F band at 1200

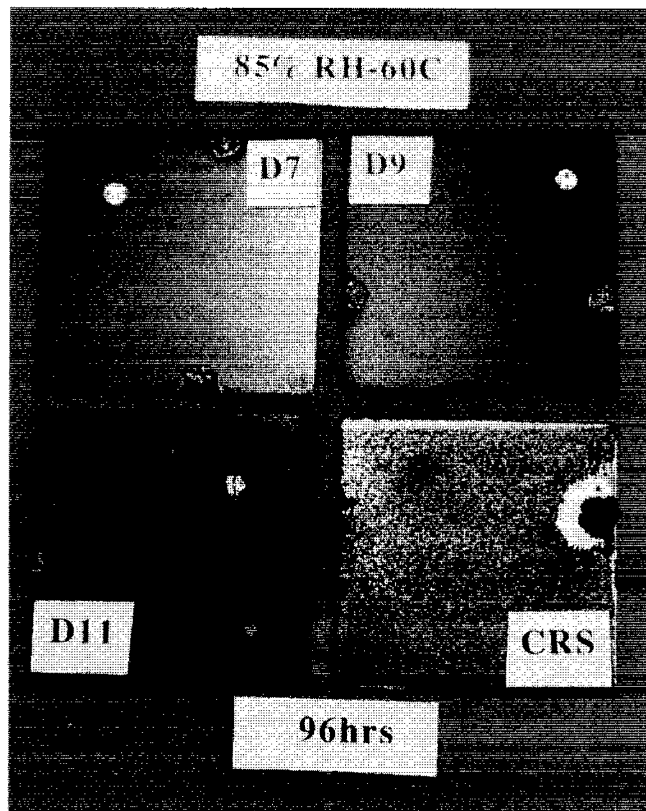

FIG. 12. Photographs of the result of the corrosion tests on the a-C:H,F coated CRS substrates.

Downloaded 17 Mar 2005 to 131.155.108.252. Redistribution subject to AIP license or copyright, see http://jap.aip.org/jap/copyright.jsp

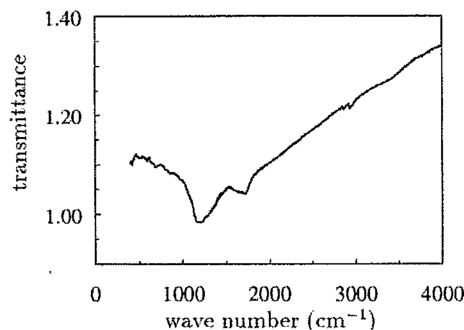

FIG. 13. Typical IR absorption spectrum of an a-C:H,F film (D9).

cm^{-1} (Ref. 38) is prominently present. In the IR spectrum of trial D7, typically hardly any absorption at all could be distinguished. Concerning the good corrosion performance of the fluorinated amorphous carbon films several explanations are possible.

(1) The partial saturation of the carbon bondings by F atoms, instead of H atoms may have led to lower internal stresses, diminishing the delamination, which would lead to direct exposure of the CRS substrate to the environment.

(2) The growth mechanism for films deposited with the use of CF_4 may be different, due to the simultaneous etching by the fluorine radicals. This view is supported by the following SEM images. In Figs. 14(a) and 14(b) images of the coatings on the silicon reference samples of trials D11 and D7 are shown. It can be observed that for D11 a typical columnar growth mechanism has occurred, which starts from island growth and results in columnar grains with curved domes on top.[40] Typical for this growth mode are the existence of voids and, corrosive species are not effectively blocked. The film deposited with CF_4 [Fig. 14(b)] appears to be very smooth. It is likely that by the simultaneous etching by the fluorine radicals and subsequent reorganization of the nanostructures, the columnar growth mechanism can be avoided. An explanation is that the mobility on the growing surface can be enhanced by a chemical mechanism.[41] The resulting film will be more uniform and dense, and provide a better anticorrosion protection.

(3) The substrate is etched by the fluorine radicals, creating a very high density of defects, which act as gettering sites, resulting in a more uniform initial growth. In the subsequent film bulk morphology the growth of large-scale separate columns is avoided. A more gradual and regular structure may arise, without or, with less voids, minimizing the diffusion of ambient air. A similar effect can be noted in the case of diamond deposition. An enhanced nucleation density on the substrate results in the growth of smoother films. In Ref. 42 successful utilization of the high etching activity of fluorine on silicon for this purpose was reported.

The growth rate in trials with CF_4 addition was of the same order as in the trials without CF_4 addition (compare ▼ and ▲ in Fig. 10). This finding implies that, in order to obtain a high quality film, the growth rate does not necessarily have to be reduced.

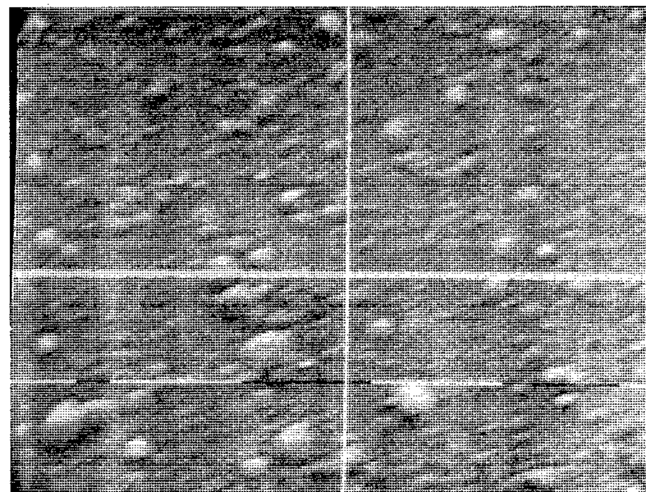

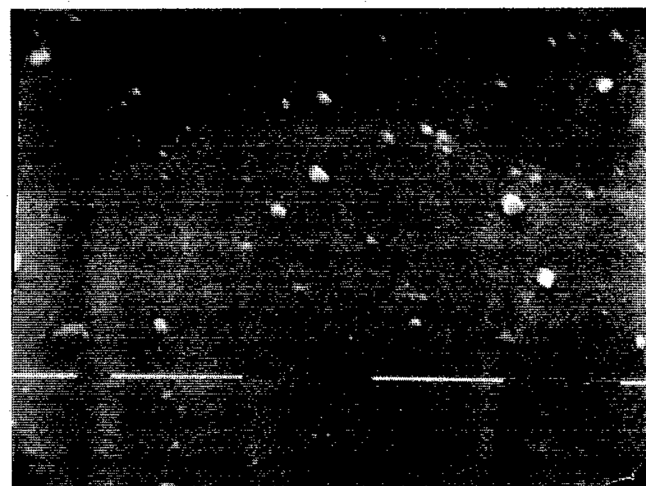

FIG. 14. SEM micrographs of an a-C:H top (D11) and an a-C:H,F film bottom (D7). A striking difference in the film structure can be noticed.

4. Results of the EIS

As a preliminary study, for the first time carbon films (on the EGS samples) were subjected to EIS. In Fig. 15 the modulus of the impedance, $\|Z\|$, is shown as a function of frequency, for various trials. The values for the best CRS films D7 and D9 however, are not very high. The highest value has been obtained for film D11. The corrosion performance of this film on CRS was low. These paradoxal results may be due to difficulties in the interpretation on the results of this novel method. Another explanation is that these results confirm the hypothesis that the growth mode on CRS is different from that on EGS. The specimen D11 was produced using toluene (meaning a relatively high Q factor), without admixture of fluorines. The only factor deviating from other trials using toluene, was the bias in the pretreatment stage. Accidently the bias was set at a high value of ~ -800V. (Obviously, this improved not only the pore resistance but also the growth rate.)

5. Results of the TOFSIMS

As a test measurement, the spectrum of a typical a-C:H film, deposited with a low hydrocarbon flow (low Q factor)

Downloaded 17 Mar 2005 to 131.155.108.252. Redistribution subject to AIP license or copyright, see http://jap.aip.org/jap/copyright.jsp

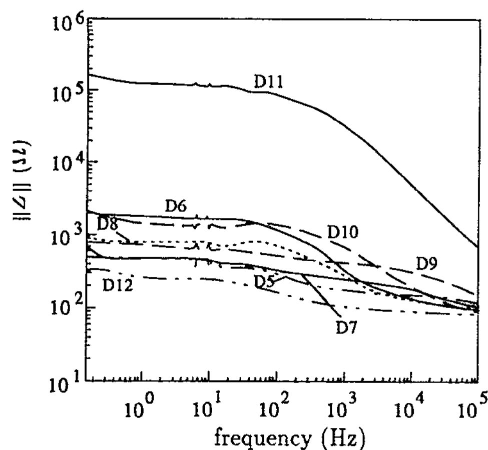

FIG. 15. EIS spectra of a-C:H,F coatings on EGS substrates.

was recorded (reactor settings approximately those of sample F2). In the positive ion spectrum, the predominant radicals in this film appeared to be C_2H_3, C_3H_5 and with a lower intensity C_2H_5, C_3H_7, C_4H_9. The former two point to an abundance of carbon sp^2 bondings over the sp^3 bonding form, indicated by the latter three species. This finding is consistent with the results of the IR measurements, which showed that low Q-factor films are more polymerlike. Some aromatic compounds were found, too. In the negative ion spectrum of this film large contaminations of oxygen and nitrogen, and also chlorine and sulphur were found. As TOFSIMS is a surface sensitive technique (upper 3 Å), this points to reactions of the top layer with the ambient air. It is known that at the surface of plasma deposited films, highly reactive free radicals occur.[34]

V. CONCLUSIONS

(1) Polymerlike and diamondlike a-C:H coatings can be deposited at high rates of tens of nm s^{-1} with the cascaded arc deposition technique using acetylene as a carrier gas. Using toluene results in the deposition of polymerlike films.

(2) In general the adhesion of the films deposited with toluene is very good, even for films with a thickness of several μm. Using acetylene results in films with a moderate adhesion.

(3) The optical and protective properties of the films can be improved by admixing additional feed gases to the argon/hydrocarbon plasma. Addition of hydrogen leads to more diamondlike films with a larger optical band gap.

(4) To obtain a high corrosion resistance, the addition of a fluorine containing gas is beneficial. Three explanations are offered:

(i) The incorporation of fluorines leads to a-C:H,F films with much smaller internal stresses compared with those of a-C:H films, and avoiding delamination.

(ii) The deposition process consists of simultaneous etching and redeposition, leading to a chemically enhanced surface mobility and a different growth morphology, resulting in a less porous structure.

(iii) By etching of the substrate by the fluorine radicals the number of sites from which the growth starts, is increased, resulting in a more uniform growth.

(5) Different film types were obtained on the CRS and the EGS substrates. On the latter the initial growth appears to require an incubation period. This may be due to the difference in (both electrical and thermal) conductivity of the substrate.

(6) The initial growth of an amorphous carbon film may be an important factor in determining the subsequent film morphology. By controlling the growth in this stage, the film properties for the bulk of the film may be predefined.

(7) A thick film is not a prerequisite for a high corrosion resistance. On the contrary, these films tend to delaminate from the substrate, providing pathways for corrosive species. Thin films are adequate and with the high growth rates obtained with the cascaded arc method, economically feasible industrial production of these films is within reach.

ACKNOWLEDGMENTS

The authors gratefully acknowledge the collaboration with Armco Research and Technology (Middletown, OH) and related laboratories, where all measurements of the corrosion study were carried out. Further they wish to thank all the persons of the Dept. of Physics, Eindhoven University of Technology who were involved in the other measurements, that is of the Surface Physics group, Professor H. H. Brongersma, Dr. C. Flipse and Dr. P. Musters, of the Nuclear Physics group, Professor M. J. A. de Voigt and Dr. L. v. IJzerndoorn, and of the EPG Plasmaphysics group, Professor F. J. de Hoog and H. den Boer, and Dr. J. J. Beulens of Daresbury Laboratory (U.K.) for the XPS measurements. The skillfull technical assistance of M. J. F. van de Sande is gratefully acknowledged.

[1] H. K. Yasuda, *Plasma Polymerization* (Academic, Orlando, 1985).
[2] J. J. Beulens, G. M. W. Kroesen, D. C. Schram, C. J. Timmermans, P. C. N. Crouzen, H. Vasmel, H. J. A. Schuurmans, C. B. Beijer, and J. Werner, J. Appl. Polym. Sci.: Appl. Polym. Symp. **46**, 527 (1990).
[3] D. C. Schram, G. M. W. Kroesen, and J. J. Beulens, J. Appl. Polym. Sci.: Appl. Polym. Symp. **46**, 1 (1990).
[4] *Plasma Deposited Thin Films*, edited by J. Mort and F. Jansen (Chemical Rubber, Boca Raton, FL, 1986).
[5] H-C. Tsai and D. B. Bogy, J. Vac. Sci. Technol. A **5**, 3287 (1987).
[6] N. I. Chapliev, T. V. Kononenko, A. A. Smolin, and V. E. Strelnitsky, Surf. Coat. Technol. **47**, 730 (1991).
[7] H. Lorenz, J. Lechner, and I. Eisele, Surf. Coat. Technol. **47**, 746 (1991).
[8] K. Enke, Mater. Sci. Forum **52/53**, 559 (1990).
[9] S. Orzesko, B. N. De, J. A. Woollam, J. J. Pouch, S. A. Alterovitz, and D. C. Ingram, J. Appl. Phys. **64**, 4175 (1988).
[10] B. Dischler, A. Bubenzer, and P. Koidl, Appl. Phys. Lett. **42**, 636 (1983).
[11] G. M. W. Kroesen, Ph.D. thesis, University of Technology, Eindhoven, The Netherlands, 1988.
[12] J. J. Beulens, Ph.D. thesis, University of Technology, Eindhoven, The Netherlands, 1991.
[13] A. J. M. Buuron, Ph.D. thesis, University of Technology, Eindhoven, The Netherlands, 1993.
[14] G. M. W. Kroesen, D. C. Schram, and M. J. F. van de Sande, Plasma Chem. Plasma Process. **10**, 49 (1990).
[15] J. J. Beulens, A. J. M. Buuron, and D. C. Schram, Surf. Coat. Technol. **47**, 401 (1991).
[16] A. J. M. Buuron, J. J. Beulens, P. Groot, J. Bakker, and D. C. Schram, Thin Solid Films **212**, 282 (1992).
[17] W. J. van Ooij, D. Surman, and H. K. Yasuda (unpublished).

Downloaded 17 Mar 2005 to 131.155.108.252. Redistribution subject to AIP license or copyright, see http://jap.aip.org/jap/copyright.jsp

[18] R. M. A. Azzam and N. M. Bashara, *Ellipsometry and Polarized Light* (North-Holland, Amsterdam, 1977).
[19] J. Robertson, Adv. Phys. **35**, 317 (1986).
[20] G. M. W. Kroesen, G. S. Oehrlein, E. de Fresart, and M. Haverlag, J. Appl. Phys. **73**, 8017 (1993).
[21] R. M. A. Driessens, Master's thesis, Internal Report No. VDF-NT 93-09 University of Technology, Eindhoven, The Netherlands, 1993.
[22] D. A. G. Bruggeman, Ann. Phys. (Leipzig) **24**, 636 (1935).
[23] J. W. Zou, K. Schmidt, K. Reichelt, and B. Dischler, J. Appl. Phys. **67**, 487 (1990).
[24] B. Dischler, A. Bubenzer, and P. Koidl, Sol. State Commun. **48**, 105 (1983).
[25] E. Gheeraert and A. Deneuville, Diamond Related Mater. **1**, 584 (1992).
[26] W. J. van Ooij, A. Sabata, and Ih-Houng Loh, European Federation of Corrosion Publications, No. 12, *Modification of Passive Films* (The Institute of Materials, London, 1994), p. 253.
[27] J. C. Pivin and T. J. Lee, Diamond Related Mater. **1**, 650 (1992).
[28] J. Koskinen, J. Appl. Phys. **63**, 2094 (1988).
[29] H. F. van Rooijen, Master's thesis, University of Technology, Eindhoven, The Netherlands, 1992.
[30] A. T. M. Wilbers, G. J. Meeusen, M. Haverlag, G. M. W. Kroesen, and D. C. Schram, Thin Solid Films **204**, 59 (1991).
[31] L. van IJzerndoorn, H. A. Rijken, S. S. Klein, and M. J. A. de Voigt, Appl. Surf. Sci. **70/71**, 58 (1993).
[32] W.-K. Chu, J. W. Mayer, and M. A. Nicolet, *Backscattering Spectrometry* (Academic, London, 1978).
[33] A. Bengtson and L. Danielsson, *Proceedings of the Sixth International Conference on Thin Films*, Stockholm, Sweden, 13–17 August 1984 (Elsevier Sequoia, The Netherlands, 1984), p. 231.
[34] W. J. van Ooij and A. Sabata, Surf. Interface Anal. **19**, 101 (1992).
[35] B. Dischler, R. E. Sah, P. Koidl, W. Fluhr, and A. Wokaun, *Proceedings of the Seventh International Symposium on Plasma Chemistry*, edited by C. J. Timmermans (Eindhoven University of Technology, The Netherlands, 1985).
[36] M. Rubin, C. B. Hopper, N.-H. Cho, and B. Bhushan, J. Mater. Res. **5**, 2538 (1990).
[37] F. Fujimoto, Jpn. J. Appl. Phys. **23**, 810 (1984).
[38] J. R. Hollahan, Th. Wydeven, and C. C. Johnson, Appl. Opt. **13**, 1844 (1974).
[39] J. J. Beulens (private communication, Daresbury Laboratory, U.K., 1993).
[40] R. Messier, J. Vac. Sci. Technol. A **4**, 490 (1986).
[41] M. J. Brett, J. Vac. Sci. Technol. A **6**, 1749 (1988).
[42] R. Rudder, Diamond Depositions: Sci. Technol. **2**, 21 (1991).

Downloaded 17 Mar 2005 to 131.155.108.252. Redistribution subject to AIP license or copyright, see http://jap.aip.org/jap/copyright.jsp